

## Electronic Supplementary Information

### Cloud-like Graphene nanoplatelets on $\text{Nd}_{0.5}\text{Sr}_{0.5}\text{CoO}_{3-\delta}$ nanorod as an Efficient Bifunctional Electrocatalyst for Hybrid Li-Air Batteries

Changmin Kim,<sup>a</sup> Ohhun Gwon,<sup>a</sup> In-Yup Jeon,<sup>a</sup> Youngsik Kim,<sup>a</sup>  
Jeeyoung Shin,<sup>b</sup> Young-Wan Ju,<sup>a,\*</sup> Jong-Beom Baek,<sup>a,\*</sup> Guntae Kim<sup>a,\*</sup>

<sup>a</sup> *Department of Energy Engineering*

*Ulsan National Institute of Science and Technology (UNIST)*

*Ulsan 44919, Republic of Korea*

<sup>b</sup> *Department of Mechanical Engineering*

*Dong-Eui University,*

*Busan 47227, Republic of Korea*

## Contents

**Fig. S1** (a) Schematic illustration and (b) photograph of a hybrid Li-air battery.

**Fig. S2** SEM images of (a) electrospun precursor nanofibers before calcination. (b) NSC nanorods after calcination at 850 °C for 4 h.

**Fig. S3** (a) ORR ring current for Pt/C, IGnP, NSC, and NSC@IGnP, respectively, in O<sub>2</sub>-saturated 0.1 M LiOH at a rotation rate of 1600 rpm and a scan rate of 0.01 V s<sup>-1</sup>. (b) peroxide yield (%).

**Fig. S4** OER polarization curves for IGnP during ten consecutive scans.

**Fig. S5** Discharge voltage profiles with different current density in a range of 625 to 2500 mA g<sup>-1</sup> in 0.1 M LiOH.

**Fig. S6** Cycling performance of Pt/C tested with hybrid Li-air battery at a current density of 125 mA g<sup>-1</sup> in 0.1 M LiOH

**Fig. S7** (a) ORR polarization curves for NSC@IGnP (1:1), NSC@IGnP (2:1), and NSC@IGnP (3:1), respectively, in O<sub>2</sub>-saturated 0.1 M LiOH at a rotation rate of 1600 rpm and a scan rate of 0.01 V s<sup>-1</sup>. (b) corresponding ring current. (c) the number of electrons transferred (n). (d) peroxide yield (%).

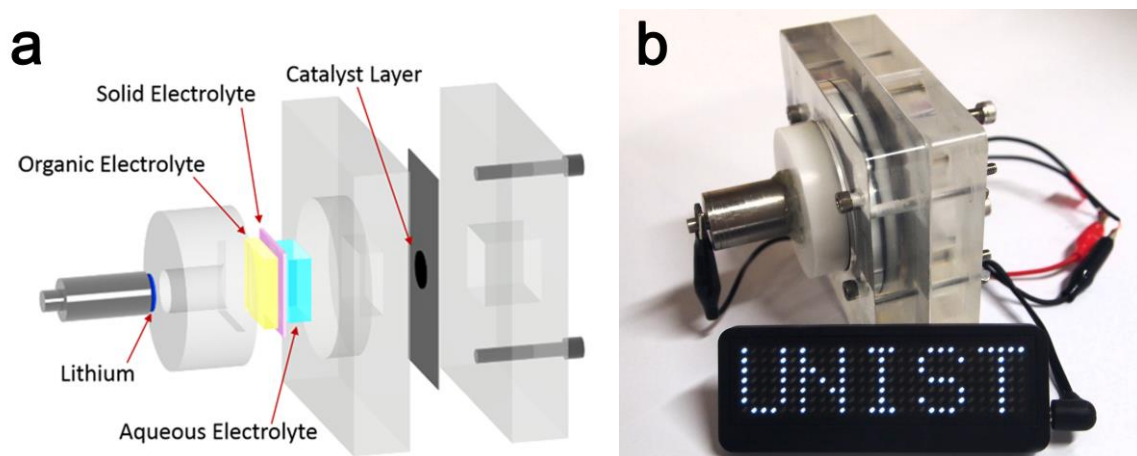


**Fig. S1** (a) Schematic illustration and (b) photograph of a hybrid Li-air battery.

Fig. S1 shows a schematic illustration and photograph of the hybrid Li-air battery. The solid electrolyte glass was first placed on the top of the anode and sealed by epoxy. Then the sealed anode was placed in an argon filled glove box where the water and oxygen concentrations were kept to less than 1 ppm. The prepared lithium metal foil disk was loaded onto the stainless steel current collector and the organic electrolyte were filled. After assembling the anode part with proper sealing, the assemblage was moved out of the glove box. The catalyst spray-coated gas diffusion layer was placed on top of the solid electrolyte and the aqueous electrolyte was filled between them. Nickel metal mesh was used as current collector onto the gas diffusion layer and electrochemical measurements were conducted on a Biologic VMP3 at ambient air condition.

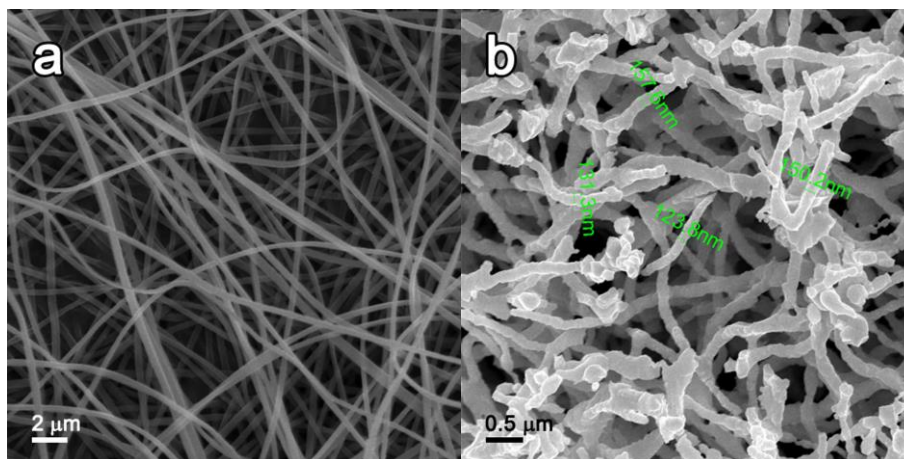


**Fig. S2** SEM images of (a) electrospun precursor nanofibers before calcination. (b) NSC nanorods after calcination at 850 °C for 4 h.

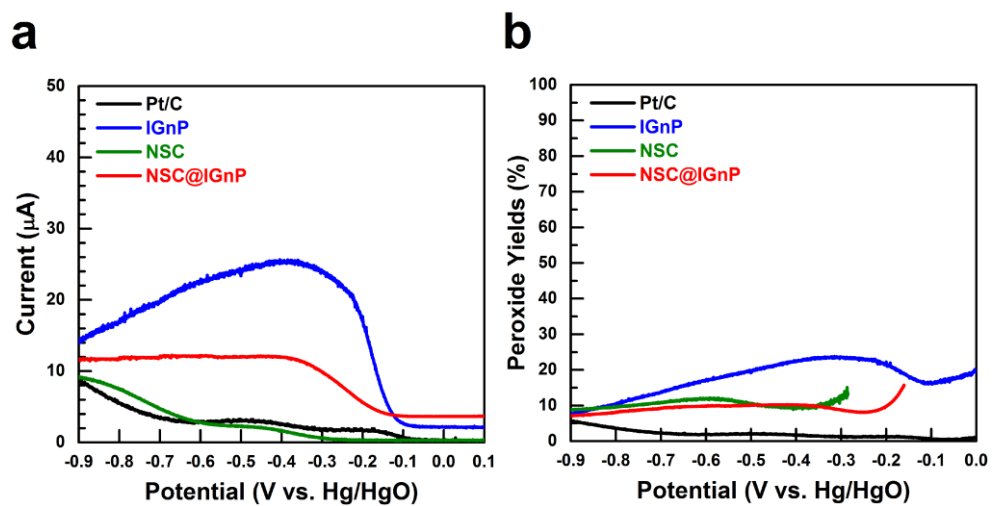


**Fig. S3** (a) ORR ring current for Pt/C, IGnP, NSC, and NSC@IGnP, respectively, in  $\text{O}_2$ -saturated 0.1 M LiOH at a rotation rate of 1600 rpm and a scan rate of  $0.01 \text{ V s}^{-1}$ . (b) peroxide yield (%).

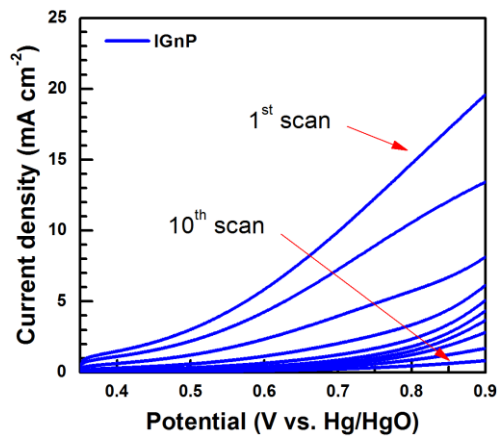


**Fig. S4** OER polarization curves for IGnP during ten consecutive scans.

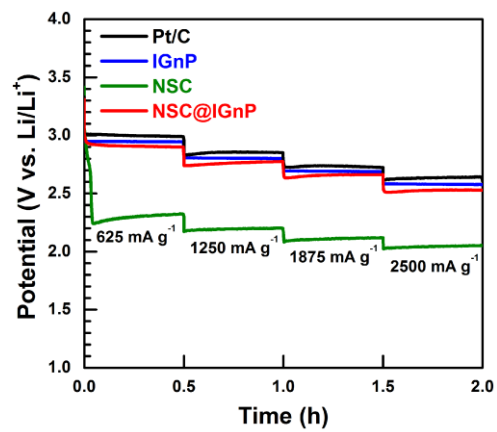


**Fig. S5** Discharge voltage profiles with different current density in a range of 625 to 2500 mA g<sup>-1</sup> in 0.1 M LiOH.

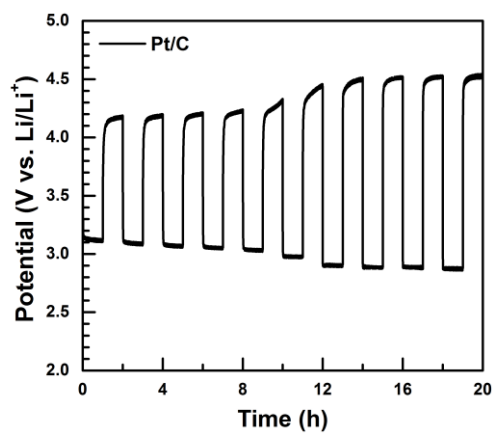


**Fig. S6** Cycling performance of Pt/C tested with hybrid Li-air battery at a current density of  $125 \text{ mA g}^{-1}$  in  $0.1 \text{ M LiOH}$



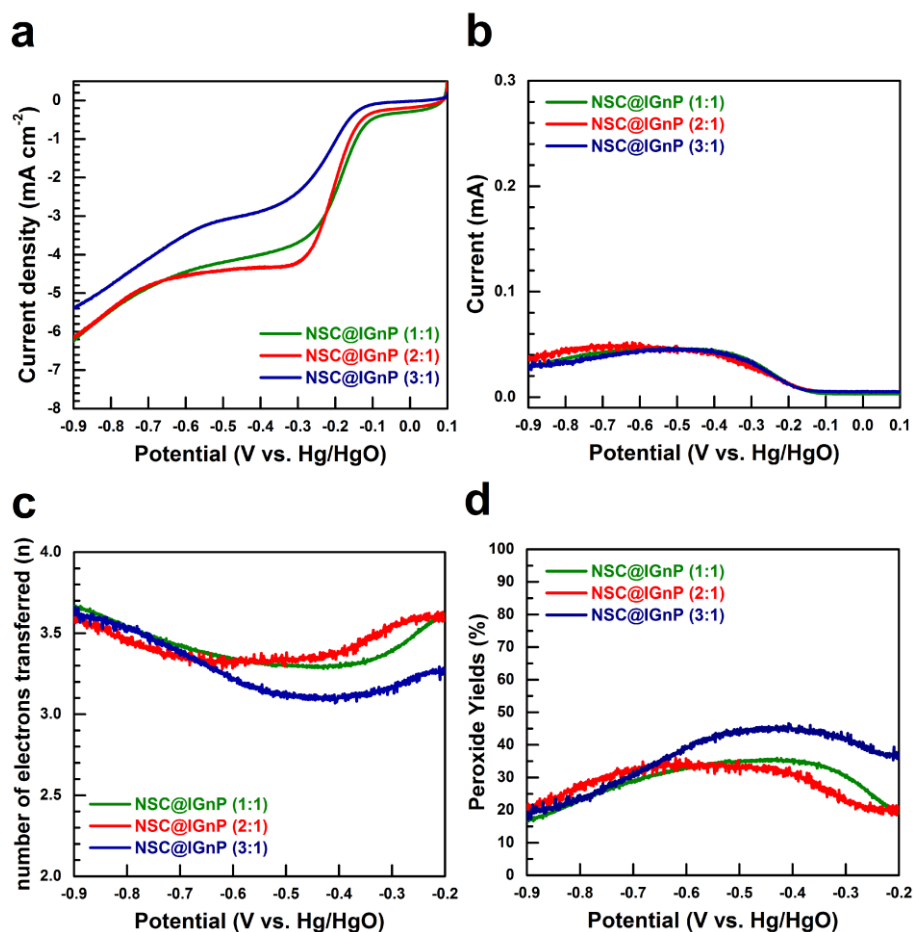


**Fig. S7** (a) ORR polarization curves for NSC@IGnP (1:1), NSC@IGnP (2:1), and NSC@IGnP (3:1), respectively, in 0.1 M LiOH at a rotation rate of 1600 rpm and a scan rate of 0.01 V s<sup>-1</sup>. (b) corresponding ring current. (c) the number of electrons transferred (n). (d) peroxide yield (%).

To find the optimum composite ratio of NSC to IGnP (*w/w*), further investigation has been carried out. With an increase in the mass ratio of NSC to IGnP, the onset potentials are negatively shifted for the ORR, as shown in Fig. S7a. This result is in accordance with observed tendency of the onset potential for each catalyst. In this work, NSC@IGnP (2:1, *w/w*) was chosen as the optimized ratio among the composites and denoted as NSC@IGnP.